

Design of Selective PAK1 Inhibitor G-5555: Improving Properties by Employing an Unorthodox Low- pK_a Polar Moiety

Chudi O. Ndubaku,^{*,†,‡} James J. Crawford,^{*,†} Joy Drobnick,[†] Ignacio Aliagas,[†] David Campbell,[‡] Ping Dong,[§] Laura M. Dornan,[†] Sergio Duron,[‡] Jennifer Epler,[†] Lewis Gazzard,[†] Christopher E. Heise,[†] Klaus P. Hoefflich,^{†,¶} Diana Jakubiak,[†] Hank La,[†] Wendy Lee,[†] Baiwei Lin,[†] Joseph P. Lyssikatos,^{†,○} Jasna Maksimoska,^{||,▽} Ronen Marmorstein,^{||} Lesley J. Murray,[†] Thomas O'Brien,[†] Angela Oh,[†] Sreemathy Ramaswamy,[†] Weiru Wang,[†] Xianrui Zhao,[†] Yu Zhong,[†] Elizabeth Blackwood,[†] and Joachim Rudolph[†]

[†]Genentech, Inc., 1 DNA Way, South San Francisco, California 94080, United States

[‡]Afraxis, Inc., 6605 Nancy Ridge Road, Suite 224, San Diego, California 92121, United States

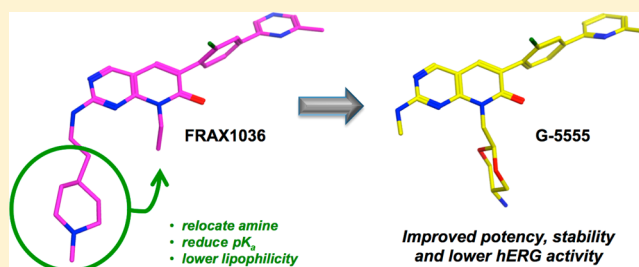
[§]Shanghai ChemPartner, 576 Libing Road, Zhangjiang Hi-Tech Park, Pudong New Area, Shanghai 201203, PRC

^{||}Perelman School of Medicine, University of Pennsylvania, 421 Curie Boulevard, Philadelphia, Pennsylvania 19104, United States

S Supporting Information

ABSTRACT: Signaling pathways intersecting with the p21-activated kinases (PAKs) play important roles in tumorigenesis and cancer progression. By recognizing that the limitations of FRAX1036 (**1**) were chiefly associated with the highly basic amine it contained, we devised a mitigation strategy to address several issues such as hERG activity. The 5-amino-1,3-dioxanyl moiety was identified as an effective means of reducing pK_a and logP simultaneously. When positioned properly within the scaffold, this group conferred several benefits including potency, pharmacokinetics, and selectivity. Mouse xenograft PK/PD studies were carried out using an advanced compound, G-5555 (**12**), derived from this approach. These studies concluded that dose-dependent pathway modulation was achievable and paves the way for further in vivo investigations of PAK1 function in cancer and other diseases.

KEYWORDS: Kinase inhibitor, oncology, hERG, pK_a



The p21-activated kinases (PAKs), which belong to the sterile-20 (STE20) family of kinases, play important roles in the regulation of key cellular phenomena including cell migration, proliferation, and survival mechanisms.¹ These kinases are located downstream of extracellular signaling molecules: integrins, receptor tyrosine kinases (RTKs), G-Protein coupled receptors (GPCRs), and immediately after specific GTPases (Rac1 and Cdc42). They mediate signal transduction through a variety of effector enzymes, proteins, and transcription factors implicated in tumorigenesis and tumor progression.^{1,2} In particular, PAK1 gene amplification and protein overexpression is associated with poor prognosis in luminal breast cancer.³ Furthermore, it was shown recently that combining a PAK1 inhibitor with docetaxel altered microtubule organization, which reduced the duration of mitotic arrest and increased the kinetics of apoptosis.⁴ As a result of these important links to cancer, there has been significant interest in the identification of potent and selective PAK1 inhibitors that are suitable for clinical development for the treatment of breast cancers as well as other tumor types.

Several PAK1 inhibitors have been described in the literature over the past few years.⁵ These include PF-3578309,⁶ previously in clinical trials but no longer progressing, and FRAX1036 (**1**, Figure 1 and Table 1).⁵ To us, compound **1** (FRAX1036) represented a good opportunity for further investigations due to a combination of high potency and moderate kinase selectivity, including selectivity over the group II PAKs. Crystal structures and molecular modeling showed that the basic amine moiety of this compound and related analogues is located in a region of the protein that lacks any specific interaction. In order to improve the binding interactions, and thereby increase the potency (and perhaps selectivity) of this class of molecules, we compared it to another PAK1 selective inhibitor that we reported recently (**2**, Figure 1).⁷ In this prior series, we found that it was possible to drive PAK1 potency and group II PAK selectivity⁵ through appending a basic amine toward a different vector within the protein, specifically directed at Asp393/Asn394, taking advantage

Received: October 9, 2015

Accepted: October 31, 2015

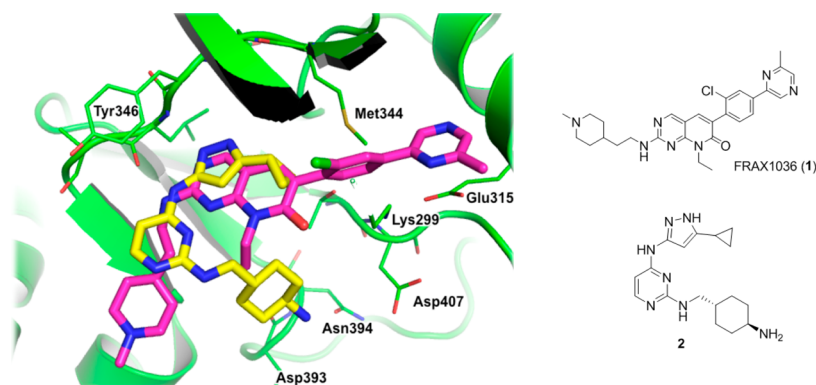
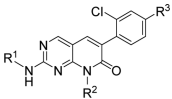


Figure 1. Overlay of FRAX1036 (**1**) (magenta, PDB: 5DFP) and aminopyrazole (**2**)⁷ (yellow, PDB: 4ZY5) in complex with PAK1, indicating a vector for improving potency by interacting with polar residues such as Asn394.

Table 1. FRAX1036 (**1**), SAR around Amine Group Transposition and “Head-Group” Changes

										
Compound	R ¹	R ²	R ³	PAK1 K _i (nM) / LLE ^a	pMEK IC ₅₀ (nM) ^b	cpKa ^c	cLogP	MDCK P _{app} ^d	hERG %inh. @ 10 μM	
1		Et		22 / 2.8	222	9.6	4.9	2.7	89	
3	Et			6.0 / 4.3	145	10.6	3.9	0.9	N.D. ^e	
4	Et			6.1 / 4.7	147	10.4	3.5	1.1	84	
5	Et			1.9 / 4.2	124	10.4	4.5	0.4	58	
6	Et			2.1 / 3.1	45	10.4	5.6	1.2	59	
7	Me			7.4 / 4.1	341	10.4	4.0	0.4	33	

^aBiochemical measurements reported are the geometric mean of ≥ 2 separate determinations; LLE = $pK_i - cLogP$. ^bCellular assay to determine the inhibition of the phosphorylation of residue S298 of MEK1 in EBC1 cells. ^cCalculated using MoKa software (version 1.1.0, Molecular Discovery). ^dCompounds were incubated with Madin–Darby canine kidney cells (MDCK) at 10 μM test concentration over 60 min; P_{app} is the rate of apical–basolateral (A–B) flux with units $\times 10^{-6}$ cm/s. ^eN.D. = not determined.

age of differing orientations of the DFG Asp motif between PAKs 1 and 4. From overlaying these structures, we postulated that a better direction to install a basic amine extension from the core of **1** was through the pyridone nitrogen. We reasoned that transposing the piperidine substituent from the aminopyrimidine portion of the core to this pyridone could allow us to increase potency of this pyridonopyrimidine class of molecules through the formation of electrostatic interaction with several polar residues in the ribose pocket of the kinase.

In going from FRAX1036 (**1**, Table 1) to the corresponding 2-ethylamino-4-piperidinylmethyl compound **3** we observed a 3.5-fold increase in potency ($K_i = 6$ nM). There was a corresponding net increase in ligand lipophilic efficiency (LLE)⁸ of 1.5. We next found that a simple linear amine extension could provide a similar potency increase, as demonstrated by compound **4**.

Furthermore, by extending the amino substituent by one atom in going to **5**, an additional potency gain of 3-fold ($K_i = 1.9$ nM) for a net >11-fold increase relative to the starting point, FRAX1036 (**1**), was achieved. Investigation of the R³ “head-group”, which binds in an induced open space near the Met344 gatekeeper, led us to settle on the 5-methyl-2-pyridinyl group (in **6**), which was equipotent to the 5-methyl-2-pyrazinyl group but showed a slight improvement in permeability (P_{app}) due to the decreased polarity. This group was found to be superior to several other heterocyclic alternatives investigated by us (data not shown). Finally, we observed that the 2-MeNH left-hand side R¹ group (**7**) offered a suitable alternative to the 2-EtNH, with a slight lowering of hERG channel inhibition. To us, this latter modification represented an advantageous change despite the small loss in potency (~3-fold) since the LLE was maintained (cf.

Table 2. PAK1 Inhibitors with Low pK_a Extensions Towards the Ribose Pocket^a

Compound	R ¹	R ²	R ³	PAK1 Ki (nM) / LLE	pMEK IC ₅₀ (nM)	cpKa	cLogP	MDCK P _{app}	hERG %inh. @ 10 μ M	HLM Cl _{hep} (mL/min kg ⁻¹) ^b
8	Et			64 / 3.8	980	4.0	3.4	21.0	22	14.7
9	Et			66 / 4.3	813	3.9	2.9	10.6	12	12.5
10	Me			19 / 5.5	399	6.9	2.2	3.5	21	10.7
11	Et			8.0 / 5.7	148	7.7	2.4	1.7	11	9.6
12 (G-5555)	Me			3.7 / 5.5	69	7.7	2.9	2.4	45	11.6
13	Me			1.9 / 5.5	57	8.4	3.2	0.4	60	13.8
14	Me			4.3 / 5.3	73	9.0	3.1	1.0	82	11.6
15	Me			7.9 / 3.6	53	7.6	4.5	N.D.	30	17.8

^aSee Table 1 for assay descriptions and abbreviations. ^bCompounds were incubated with human liver microsomes for 1 h, and % remaining was determined by LC–MS/MS analysis.

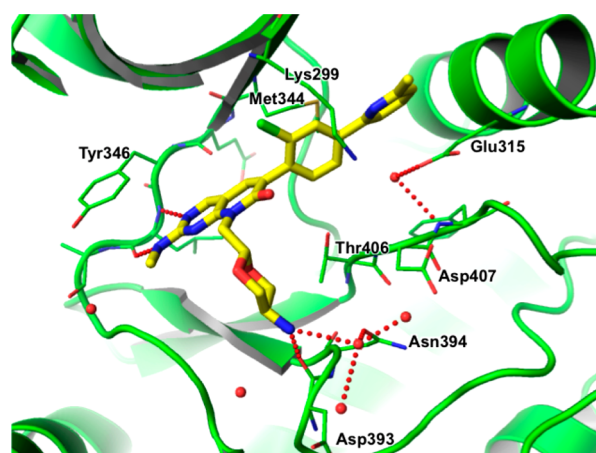


Figure 2. Co-crystal structure of G-5555 (12) in complex with PAK1 (PDB: SDEY). Hydrogen-bonding interactions are shown as dotted red lines. Water molecules appear as red spheres.

5 and 7). It was clear that an amine moiety was able to drive potency, presumably by interacting with the negatively charged or polar oxygen residues (e.g., Asp393, Asn394, and Asp407) in this region of the kinase. This polar pocket normally accommodates the ribose sugar portion of the endogenous substrate, ATP.

The next question we addressed was whether we required such basic amines (i.e., with calculated $pK_a > 10$)⁹ to achieve the observed level of potency. In particular, we were concerned that high pK_a when coupled with high cLogP would lead to greater activity against ion channels, such as the hERG voltage-gated potassium channel.¹⁰ This liability can often be mitigated by reducing the pK_a of a molecule or by reducing its lipophilicity,^{11,12} and sometimes, greater reductions can be achieved if both properties are reduced simultaneously.^{13,14} Indeed, we found compound 1 to show strong hERG inhibition (89%) when tested at 10 μ M in a patch clamp assay (Table 1). Another issue with this initial set of compounds was that permeability, measured using Madin–Darby canine kidney epithelial cells (MDCK), was poor (e.g., $P_{app} = 1.2 \times 10^{-6}$ cm/s for 6). Overall, these compounds clearly lacked the required levels of permeability to achieve good cellular activity and oral absorption.

We set out to address these concerns by reducing both the pK_a and the lipophilicity of our molecules (Table 2). Again, we focused on the R² amine-containing portion of the molecule that binds within the ribose pocket of PAK1. Removing the basic amine moiety (Table 2, compounds 8 and 9) resulted in a dramatic reduction in biochemical activity and a corresponding activity drop in the mechanistic cellular assay (in this case, measuring phosphorylation levels of a PAK1-specific down-

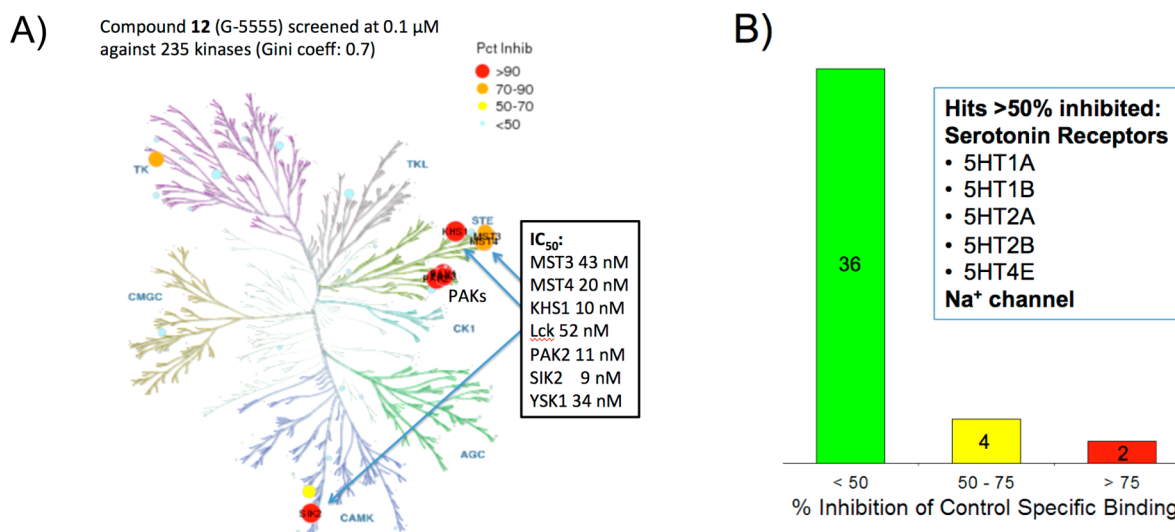


Figure 3. Selectivity profile of compound **12**. (A) Kinome tree diagram illustrating its kinase selectivity determined at 0.1 μ M (Invitrogen). IC₅₀ values shown for kinases inhibited >70% other than PAK3 (IC₅₀ not determined). (B) Bar chart illustrating the number of off-targets of **12** determined in a secondary pharmacology screening panel (compound concentration = 10 μ M). Green, inhibition <50%; yellow, inhibition between 50 and 75%; red, inhibition >75%. The numbers indicate the counts contained within each bin. See [Supporting Information](#) for more details.

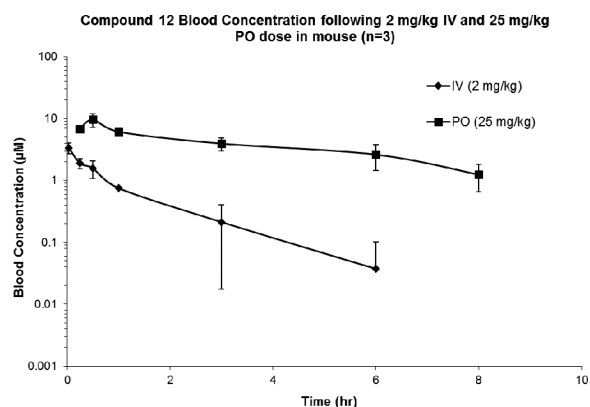


Figure 4. Concentration–time curve of **12** dosed i.v. (2 mg/kg) or p.o. (25 mg/kg). Each curve represents mean values measured for three mice.

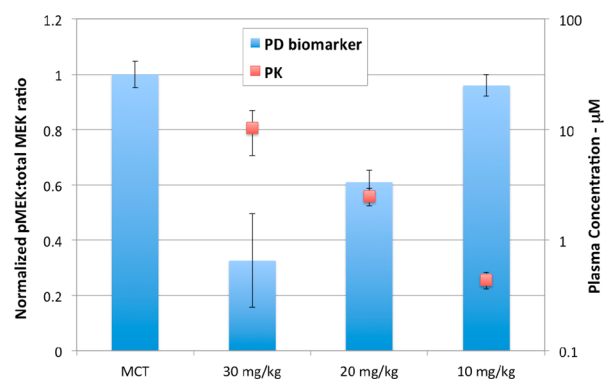


Figure 5. Bar chart indicating dose response PK/PD of pMEK level suppression with compound **12** at 10, 20, and 30 mg/kg in H292-xenograft mice versus MCT vehicle (mean \pm SEM is graphed). See [Supporting Information](#) for further details.

stream target, pMEK S298). These results suggested that strong polar interactions in this area were indeed crucial for driving potency. One way to attenuate the pK_a and lipophilicity of

amines is through the inductive effects of oxygen atoms placed in close proximity to the nitrogen. We saw that employing the R² morpholine extension in **10** (calculated pK_a = 6.9) resulted in reasonable biochemical potency (K_i = 19 nM), albeit still showing weak activity in cells (pMEK IC₅₀ = 399 nM). Reassuringly, the permeability of this compound was improved (P_{app} = 3.5 \times 10⁻⁶ cm/s), and the hERG activity was reduced (21% inhibition at 10 μ M test concentration). Next, an atypical 5-amino-1,3-dioxanyl moiety (compound **11**, [Table 2](#)) was introduced, which served to mimic the highly potent 4-aminocyclohexane in compound **5** in [Table 1](#). Although 1,3-dioxanes are not commonly found in active pharmaceutical agents due to their perceived instability, our choice to use this particular group was inspired by the fact that the proximal amine group serves to “protect” the sensitive acetal functionality against protonolysis.^{15,16} Through adding two geminal oxygen atoms the substituent remains meso, thereby minimizing stereochemical complexity. Furthermore, the inductive effect of having two oxygen atoms β to the amine has the benefit of reducing its basicity to a desirable range (calculated pK_a = 7.7 for **11**). Finally, the clogP of this analogue was reduced by greater than two units. Due to a valid concern about the stability of such a group, we undertook a series of forced degradation experiments with **11** and found this compound to be stable.¹⁷ Additionally, the in vitro stability in liver microsomes was comparable to (or better than) previous compounds evaluated (HLM CL_{hep} = 9.6 mL/min/kg). To build upon the advantages offered by **11**, we sought to improve upon its permeability and cellular potency.

To this end, some of the features that previously had been shown to be beneficial were introduced to this molecule. This included refinement of the left-hand side group to a 2-MeNH group (instead of 2-EtNH) and the right-hand side to a methylpyridine (replacing the methylpyrazine). These efforts led to the identification of compound **12** (G-5555), which was potent, showing good activity in the pMEK cellular assay, had improved permeability, and importantly, displayed low hERG channel activity (<50% inhibition at 10 μ M).^{17,18} N-Methylation of the amino group (**13**) in an attempt to further increase permeability by reducing H-bond donors did not provide any

benefit. Other low pK_a designs were also evaluated (compound **14** and the difluorinated compound **15**¹⁹), but none of these changes provided a compound with an improved profile relative to **12**.

Next, the X-ray crystal structure of **12** in PAK1 was determined (Figure 2). The structure confirmed that the binding mode of **12** was indeed as expected. The methylpyridine “head-group” binds in the pocket bordered by the α C-helix (with Glu315 stacking interaction), catalytic Lys299, and gatekeeper Met344. The rest of the core scaffold adopts an orientation similar to FRAX1036 (PDB: 5DFP) with two H-bond interactions at the hinge. The newly introduced 5-amino-1,3-dioxanyl motif makes a bifurcated H-bond interaction with backbone carbonyl of Asp393 and a water molecule, which in turn makes a hydrogen bond with the side chain of Asn394. Interestingly, the two annular oxygen atoms are not making any observable interactions within the binding pocket.

Having identified compound **12**, we proceeded to further characterize its selectivity and in vitro safety profile (Figure 3). First, the kinase selectivity of **12** was determined against a panel of 235 kinases (screened at 0.1 μ M concentration equal to 58-fold above PAK1 K_i). Compound **12** showed excellent kinase selectivity and inhibited only eight out of the 235 kinases tested other than PAK1 with inhibition >70%: PAK2, PAK3, KHS1, Lck, MST3, MST4, SIK2, and YSK1. The IC_{50} of **12** against these kinases was determined, and the values are shown in Figure 3A.¹⁷ In general, the compound demonstrated high selectivity for the group I PAKs. In addition, a secondary pharmacology screen against a panel of receptors, transporters, ion channels, and enzymes²⁰ showed remarkable lack of activity, only inhibiting the serotonin receptors (5HT1A, 5HT1B, 5HT2A, 5HT2B, and 5HT4E) and the Na⁺ channel >50% (Figure 3B). These results are in contrast to the activity of FRAX1036 in the same screen, which showed significant activity against a majority of the receptors and channels tested (data not shown). Crucially, there was negligible activity for **12** against the hERG channel with IC_{50} > 10 μ M in a patch clamp assay.

To assess the in vivo pharmacokinetic behavior of **12**, we dosed female CD-1 mice with either 2 mg/kg intravenously (i.v.) or 25 mg/kg orally (p.o.) and monitored compound blood concentrations over 8 h (Figure 4). Low blood clearance (CL_{blood} = 24.2 mL/min/kg) and an acceptable half-life ($t_{1/2}$ = 53 min) were observed.¹⁷ Additionally, good oral exposure (AUC = 30 μ M·h) and high oral bioavailability (F = 80%) were achieved. Taken together, these data indicated that we could achieve sufficiently sustained levels of **12** to study target modulation and pathway suppression in vivo. Moreover, in PK studies conducted in cynomolgus monkey, compound **12** showed low clearance (CL_p = 3.4 mL/min/kg) and high oral bioavailability (F = 72%).¹⁷ These results suggest a potential for good human exposure if the compound was advanced to the clinic.

To study target modulation in vivo, nude mice bearing H292 NSCLC xenografts were administered a range of three doses (10, 20, and 30 mg/kg) of **12**.¹⁷ Tumors and blood were collected at 6 h postdose and analyzed for circulating drug levels and alterations in the pharmacodynamic biomarker (pMEK S298). Drug dose- and exposure-dependent reductions in pMEK were consistent with the cellular potency and pharmacology of **12** (Figure 5).

In conclusion, in starting from an advanced PAK1 inhibitor, FRAX1036, we were able to optimize the binding mode and substituents, allowing us to ultimately balance potency, permeability, and hERG activity. We postulated that the highly

basic amine extension on the compound was a likely cause of these unfavorable attributes. To improve on these limitations, we designed the 5-amino-1,3-dioxanyl group that helped to lower the pK_a and cLogP and ultimately derived **12**. This optimized compound demonstrated in vivo PK/PD effects consistent with the observed potency and pharmacokinetic properties. We are currently utilizing this molecule to further study PAK1 function in cancer and other disease contexts.

■ ASSOCIATED CONTENT

Supporting Information

The Supporting Information is available free of charge on the ACS Publications website at DOI: 10.1021/acsmchemlett.5b00398.

Pharmacokinetic and pharmacodynamic study protocols, protein production and crystallographic information, assay protocols, compound synthesis, and characterization (PDF)

■ AUTHOR INFORMATION

Corresponding Authors

*(C.O.N.) Tel: 510-809-9290. E-mail: cndubaku@aduro.com.

*(J.J.C.) Tel: 650-467-8886. E-mail: crawfoj5@gene.com.

Present Addresses

[†]Aduro Biotech, 626 Bancroft Way, 3C, Berkeley, California 94710, United States.

[#]Blueprint Medicines, 215 First Street, Cambridge, Massachusetts 02142, United States.

[○]Biogen, 225 Binney Street, Cambridge Massachusetts 02142, United States.

[▽]Janssen R&D, LMAD, 200 Great Valley Parkway, Malvern, Pennsylvania 19355, United States.

Author Contributions

The manuscript was written through contributions of all authors. All authors have given approval to the final version of the manuscript.

Funding

Diffraction data were collected at beamline 08ID-1 at the Canadian Light Source, which was supported by the NSERC, the NRC, the Canadian Institutes of Health Research, the Province of Saskatchewan, Western Economic Diversification Canada, and the University of Saskatchewan at beamline 5.0.2 of the Advanced Light Source. The Berkeley Center for Structural Biology was supported in part by the NIH, the NIGMS, and the Howard Hughes Medical Institute. The Advanced Light Source was supported by the Director, Office of Basic Energy Sciences, of the U.S. Department of Energy under Contract No. DE-AC02-05CH11231.

Notes

The authors declare the following competing financial interest: J.J.C., J.D., I.A., J.E., L.G., C.E.H., D.J., H.L., W.L., B.L., L.J.M., T.O., A.O., S.R., W.W., X.Z., Y.Z., E.B., and J.R. are employees and stockholders of Roche.

■ ACKNOWLEDGMENTS

We thank A. Guillen, B. Murphy, M. Wong, Y. Liu, and D. Wang (Genentech) for compound purification and analytical support. We also thank D. Favor (Shanghai ChemPartner) for helpful discussions.

■ ABBREVIATIONS

Cdc42, cell division control protein 42 homologue; HLM, human liver microsomes; LLE, ligand lipophilic efficiency; MCT, methylcellulose/Tween; PAK, p21-activated kinase; P_{app} , apparent permeability; pMEK, phosphorylated mitogen-activated protein kinase kinase; SEM, standard error of the mean

■ REFERENCES

- (1) Radu, M.; Semenova, G.; Kosoff, R.; Chernoff, J. Pak Signaling in the Development and Progression of Cancer. *Nat. Rev. Cancer* **2014**, *14*, 13–25.
- (2) Zhao, Z.-S.; Manser, E. PAK Family Kinases: Physiological Roles and Regulation. *Cellular Logistics* **2012**, *2*, 59–68.
- (3) Ong, C. C.; Jubb, A. M.; Haverty, P. M.; Zhou, W.; Tran, V.; Truong, T.; Turley, H.; O'Brien, T.; Vucic, D.; Harris, A. L.; Belvin, M.; Friedman, L. S.; Blackwood, E. M.; Koeppen, H.; Hoeflich, K. P. Targeting p21-Activated Kinase 1 (PAK1) to Induce Apoptosis of Tumor Cells. *Proc. Natl. Acad. Sci. U. S. A.* **2011**, *108*, 7177–7182.
- (4) Ong, C. C.; Gierke, S.; Pitt, C.; Sagolla, M.; Cheng, C. K.; Zhou, W.; Jubb, A. M.; Strickland, L.; Schmidt, M.; Duron, S. G.; Campbell, D. A.; Zheng, W.; Dehdashti, S.; Shen, M.; Yang, N.; Behnke, M. L.; Huang, W.; McKew, J. C.; Chernoff, J.; Forrest, W. F.; Haverty, P. M.; Chin, S.-F.; Rakha, E. A.; Green, A. R.; Ellis, I. O.; Caldas, C.; O'Brien, T.; Friedman, L. S.; Koeppen, H.; Rudolph, J.; Hoeflich, K. P. Small Molecule Inhibition of Group I p21-Activated Kinases in Breast Cancer Induces Apoptosis and Potentiates the Activity of Microtubule Stabilizing Agents. *Breast Cancer Res.* **2015**, *17*, 59–70.
- (5) For a recent review, see: Rudolph, J.; Crawford, J. J.; Hoeflich, K. P.; Wang, W. Inhibitors of p21-Activated Kinases (PAKs). *J. Med. Chem.* **2015**, *58*, 111–129.
- (6) Murray, B. W.; Guo, C.; Piraino, J.; Westwick, J. K.; Zhang, C.; Lamerdin, J.; Dagostino, E.; Knighton, D.; Loi, C.-M.; Zager, M.; Kraynov, E.; Popoff, I.; Christensen, J. G.; Martinez, R.; Kephart, S. E.; Marakovits, J.; Karlicek, S.; Bergqvist, S.; Smeal, T. Small-Molecule p21-Activated Kinase Inhibitor PF-3758309 Is a Potent Inhibitor of Oncogenic Signaling and Tumor Growth. *Proc. Natl. Acad. Sci. U. S. A.* **2010**, *107*, 9446–9451.
- (7) Crawford, J. J.; Lee, W.; Aliagas, I.; Mathieu, S.; Hoeflich, K. P.; Zhou, W.; Wang, W.; Rouge, L.; Murray, L.; La, H.; Liu, N.; Fan, P. W.; Cheong, J.; Heise, C. E.; Ramaswamy, S.; Mintzer, R.; Liu, Y.; Chao, Q.; Rudolph, J. Structure-Guided Design of Group I Selective p21-Activated Kinase Inhibitors. *J. Med. Chem.* **2015**, *58*, 5121–5136.
- (8) Tarcsay, Á.; Nyíri, K.; Keserű, G. M. Impact of Lipophilic Efficiency on Compound Quality. *J. Med. Chem.* **2012**, *55*, 1252–1260 and references therein.
- (9) Calculated using MoKa software (version 1.1.0, Molecular Discovery).
- (10) Redfern, W. S.; Carlsson, L.; Davis, A. S.; Lynch, W. G.; MacKenzie, I.; Palethorpe, S.; Siegl, P. K. S.; Strang, I.; Sullivan, A. T.; Wallis, R.; Cramm, A. J.; Hammond, T. G. Relationships Between Preclinical Cardiac Electrophysiology, Clinical QT Interval Prolongation and Torsade De Pointes for a Broad Range of Drugs: Evidence for a Provisional Safety Margin in Drug Development. *Cardiovasc. Res.* **2003**, *58*, 32–45.
- (11) Braga, R. C.; Alves, V. M.; Silva, M. F. B.; Muratov, E.; Fourches, D.; Tropsha, A.; Andrade, C. H. Tuning HERG Out: Antitarget QSAR Models for Drug Development. *Curr. Top. Med. Chem.* **2014**, *14*, 1399–1415.
- (12) Aronov, A. M. Tuning Out of hERG. *Curr. Opin. Drug Discovery Dev.* **2008**, *11*, 128–135.
- (13) Kawai, Y.; Tsukamoto, S.; Ito, J.; Akimoto, K.; Takahashi, M. A Risk Assessment of Human Ether-a-Go-Go-Related Gene Potassium Channel Inhibition by Using Lipophilicity and Basicity for Drug Discovery. *Chem. Pharm. Bull.* **2011**, *59*, 1110–1116.
- (14) Peters, J.-U.; Schnider, P.; Mattei, P.; Kansy, M. Pharmacological Promiscuity: Dependence on Compound Properties and Target Specificity in a Set of Recent Roche Compounds. *ChemMedChem* **2009**, *4*, 680–686.
- (15) Houben-Weyl: Science of Synthesis, 26.1.6.6.1, Hydrolysis of O,O-Acetals, p 333.
- (16) Bi, L.; Zhao, M.; Gu, K.; Wang, C.; Ju, J.; Peng, S. Toward the Development of Chemoprevention agents (III): Synthesis and Anti-Inflammatory Activities of a New Class of 5-Glycylamino-2-substituted-phenyl-1,3-dioxacycloalkanes. *Bioorg. Med. Chem.* **2008**, *16*, 1764–1774.
- (17) See [Supporting Information](#) for more details.
- (18) Inhibition curve was determined showing hERG $IC_{50} > 10 \mu M$ in ChanTest patch clamp assay.
- (19) For a recent review of fluorine in medicinal chemistry, see: Gillis, E. P.; Eastman, K. J.; Hill, M. D.; Donnelly, D. J.; Meanwell, N. A. Applications of Fluorine in Medicinal Chemistry. *J. Med. Chem.* **2015**, DOI: [10.1021/acs.jmedchem.5b00258](https://doi.org/10.1021/acs.jmedchem.5b00258).
- (20) Compound **12** was screened at $10 \mu M$ against a panel of 42 representative receptors, transporters, ion channels, and enzymes at CEREP.